The effects of pH, ionic strength, and iron–fulvic acid interactions on the kinetics of non-photochemical iron transformations. II. The kinetics of thermal reduction

MICHAEL J. PULLIN[1],* and STEPHEN E. CABANISS[2]

[1]Department of Civil Engineering and Geological Sciences, University of Notre Dame, Notre Dame, IN 46556, USA
[2]Department of Chemistry, University of New Mexico, Albuquerque, NM 87131, USA

Abstract—A combination of flow-injection analysis and kinetic analysis was used to examine the speciation of iron(II) and iron(III) in fulvic acid solutions as a function of pH, ionic strength, and time. This methodology was used to follow a shift in iron speciation from faster to slower reacting species over a timescale of several days. This speciation data shows that both iron(II) and iron(III)–fulvic acid complexes are important iron species in humic-containing natural waters and that their amounts and their rates of transformation to colloidal iron are controlled primarily by the kinetics of thermal (dark) reduction and iron(II) oxidation. The kinetic analysis methodology also yielded the rate constants for the thermal reduction of iron by the fulvic acid. These rate constants decrease with increasing pH and are independent of ionic strength. While thermal reduction was found to be too slow to produce large amounts of steady state iron(II) at circumneutral pH, it does provide a mechanism for iron redox cycling in the absence of photochemical or biochemical processes.   *Copyright © 2003 Elsevier Ltd*

1. INTRODUCTION

The non-photochemical, abiotic reactions of iron in natural waters include iron(II) oxidation, iron colloid formation, iron(II)- and iron(III)-dissolved organic matter (DOM) complexation and dissociation, and the thermal or "dark" reduction of iron by DOM. These processes can all occur on roughly the same timescale, creating an interdependent network of reactions that control the speciation of iron in natural waters. While previous work has focused on photochemical and biochemical iron(III) reduction, studies that examine the thermal iron(III) reduction by natural organic matter have been few.

In the previous companion paper (Pullin and Cabaniss, 2003), a study of the effect of DOM on the kinetics of iron(II) oxidation indicated that this thermal iron(III) reduction reaction might be important in determining iron speciation in iron-DOM systems. Iron(II) oxidation experiments in the presence of DOM at pH 6.0 showed that some back-reaction of the iron(III)-oxidation product to form iron(II) was probably occurring. To follow up on this possibility, this study was undertaken to specifically measure the rates of thermal reduction and to determine its effect on iron speciation.

The thermal reduction of iron(III) by fulvic acid has been noted by a number of researchers (Waite and Morel, 1984; Voelker and Sulzberger, 1996; Emmenegger et al., 2001). Voelker and Sulzberger (1996) found that Suwannee River fulvic acid rapidly reduced iron(III) at pH 3 and 5 in the dark. They observed an initially fast reduction, followed by a slower process, suggesting either multiple binding sites or a slow rearrangement of the fulvic acid to form stronger complexes.

Emmenegger et al. (2001) also noted thermal reduction and noted that it was stimulated by light exposure. This was attributed to the photochemical formation of superoxide and/or

DOM carbon radicals, which continued to act as an iron(III) reductant after irradiation ceased. They observed no iron(II) in samples that had never been exposed to light. However, their direct iron(II) measurements would only have detected the net iron(II) produced at a rate faster than the oxidation of iron(II), leaving open the question of whether or not thermal reduction induced redox cycling occurs in the absence of light-exposure at circumneutral pH values. Nevertheless, the work of Emmenegger et al. (2001) does suggest that the reaction of these organic matter-derived radical species may be the underlying chemical mechanism for thermal reduction. An additional or alternative possible mechanism is the reaction of iron(III) with quinone (i.e., Scott et al., 1998) or catechol-type functional groups present in these substances (Stumm and Morgan, 1981).

In this study, to better understand the magnitude of thermal reduction and its effect on iron speciation, kinetic analysis was used to measure both the rate constants for this process and its effect on iron-DOM speciation. This first use of this approach to study iron-DOM speciation was by Langford and coworkers, who used kinetic analysis with iron(II) and iron(III)-specific colorimetric ligands to measure the distribution of iron species in fulvic acid-containing model solutions (Langford and Khan, 1975; Langford et al., 1977, 1981). They found evidence for iron(III) complexation by humic materials and reported the formation of iron(II) from the thermal reduction of iron(III) by a fulvic acid. Based on differing reduction rates, they concluded that multiple iron(III)–fulvic acid species must exist. Waite and Morel (1984), also using kinetic analysis, found evidence for multiple iron(III)–fulvic acid species and were able to show that one of these complexes acted as a primary chromophore, producing iron(II) under illumination.

While these studies have improved our understanding of iron-DOM interactions, they have also left unanswered questions. One major difficulty is that the laboratory studies described above generally allow a fixed amount of time for the iron and fulvic acid to interact before beginning the kinetic

---

* Author to whom correspondence should be addressed (mpullin@nd.edu).

analysis to determine the iron speciation. However, it is possible that the distribution of iron species will change over hours and days, perhaps affecting the overall rate of thermal reduction. A second limitation is that most of the laboratory experiments were conducted at pH values ≤ 6.5 and at a single ionic strength. An additional concern is the interpretation of the reactivity of iron(III)-DOM solutions to the iron(II) binding ligands (ferrozine and 1,10 phenanthroline) frequently used for kinetic analysis. The reduction of iron(III) in the presence of DOM and the iron(II)-specific ligand could be the result of either the thermal reduction of iron(III) by DOM or the induced reduction of iron(III) upon the binding of iron(II) by the ligand. The second possibility would imply that the reductive process observed by the studies discussed above is simply an artifact of the analysis technique employed.

The research presented here examines the effect of thermal reduction on the speciation of iron in iron-DOM solutions. Initial experiments validate the use of ferrozine for measuring iron(II) in the presence of iron(III) and the use of kinetic analysis for measuring iron(II) reduction rates, although only under certain conditions. Once this methodology is established, the various species of iron present in iron–fulvic acid solutions are quantified using kinetic analysis as a function of the time elapsed after mixing iron(II) or iron(III) with pH and ionic strength buffered fulvic acid solutions. The kinetic analysis data are supplemented with independent measurements of iron(II) and colloidal iron. The effects of pH, ionic strength, and iron redox state on thermal reduction kinetics were all quantitatively examined for systems which approximate fresh natural waters.

2. EXPERIMENTAL

2.1. Materials

Glacial acetic acid (trace metal grade), sodium hydroxide (99.99%), sodium perchlorate, 3-(2-pyridyl)-5,6-diphenyl-1,2,4-triazine-p,p'-disulfonic acid (ferrozine), redistilled (99.999+%) 70% nitric acid, a 1000-μg/mL iron AA/ICP standard and the hemisodium salts of 2-(N-morpholino)ethanesulfonic acid (MES) and N-(2-hydroxyethyl)piperazine-N'-(2-ethanesulfonic acid) (HEPES) were obtained from the Sigma-Aldrich Chemical Co. Suwannee River fulvic acid (SRFA) was provided by Jerry Leenheer (U.S. Geological Survey, CO). Citric acid (p.a.) and certified ACS grade ferrous ammonium sulfate hexahydrate was obtained from Fisher Scientific. before use, the iron(II) salt was warmed in an oven at 45°C for 1 h and stored in a desiccator until use. All other chemicals were used as provided. Deionized water (≥17.8 MΩ) was used throughout.

2.2. Iron–Fulvic Acid Solution Preparation

To make the iron–fulvic acid solutions analyzed in these experiments, pH 6.0 (MES) or 8.0 (HEPES) buffer, SRFA, and sodium perchlorate (when used) were added from concentrated stock solutions to a 50 mL polypropylene volumetric flask, diluted to ~40 mL with deionized water, and mixed thoroughly. Next, either iron(II) from a freshly made ferrous ammonium sulfate stock solution (pH 2.0 from HNO$_3$) or iron(III) from the AA/ICP standard (1–2 wt.% HNO$_3$) was added, a timer was started, and the solution was diluted to volume and mixed again. The final concentrations were as follows: 10.0 mmol/L buffer, 10.0 mg/L fulvic acid, 0.10 mol/L sodium perchlorate (when used), and 10.0 μM total iron. For each kinetic analysis experiment, a control solution was made in the same manner but without any added iron. The solution preparation and analysis were conducted in near darkness, with only the dim light from computer monitors and instrument displays present. The sample flasks were wrapped in aluminum foil once the final dilution and mixing were complete, further limiting

exposure to light. The solutions were stored in complete darkness during incubation. Polypropylene volumetric flasks (Nalgene), PTFE beakers, and polymeric pipetter tips were used for the handling of all iron-containing solutions.

2.3. Kinetic Analysis for the Determination of Iron Speciation

2.3.1. Kinetic analysis theory

The kinetic analysis method allows a set of metal species to undergo ligand exchange with an added excess of strong-binding ligand to form a single, measurable, common product (Ridder and Margerum, 1977). Ideally, each species initially present in solution will exchange at a different rate. The resulting common product concentration vs. time data can then be numerically fit as the sum of pseudo-first order parallel reactions, one reaction for each species present in the sample. The fitting process yields two parameters for each species, an initial concentration and a rate constant. The combined initial concentrations of all the metal-ligand complexes represent the metal's speciation at the time the kinetic analysis experiment began.

The physical meaning of a rate constant measured by kinetic analysis depends on the type of ligand exchange mechanism occurring (Langford and Gray, 1965; Hering and Morel, 1988, 1990). For the disjunctive pathway, the original metal complex (ML) dissociates before the second added ligand (L′) binds the metal (Hering and Morel, 1990):

$$ML + L' \rightleftharpoons M + L + L' \rightleftharpoons ML' + L \qquad (1)$$
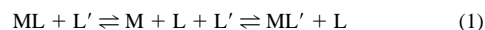
In this case, the dissociation (first) step is generally the rate limiting step. When [L′] ≫ [L], the second step is essentially irreversible, leading to a "trapping" of the metal as it dissociates from the original complex (Hering and Morel, 1990). Under these conditions, the concentration of the added ligand ([L′]) has no effect on the observed rate and the reaction is first-order with respect to ML (Olsen and Shuman, 1985). A ligand exchange reaction proceeds by an adjunctive pathway if the initial step is attack of the original complex by the added ligand, followed by dissociation of the resulting ternary complex (Hering and Morel, 1990):

$$ML + L' \rightleftharpoons L'ML \rightleftharpoons ML' + L \qquad (2)$$

In this case, the observed rate is dependent on [L′] (Hering and Morel, 1990).

As long as [L′] ≫ [L], the effect of changing the concentration of L′ on the observed rate can be used to determine which mechanism is occurring in the ligand exchange. When it can be shown that ligand exchange occurs by a disjunctive mechanism (independent of [L′]), the measured rate constant for the reaction is the conditional rate constant for the dissociation of the original metal-ligand complex (Olsen and Shuman, 1985).

While kinetic analysis yields the concentration (and possibly a reaction rate) for each species present at the time L′ is added, it does not indicate whether a steady state distribution of species has been reached at that time. The time between mixing the metal and ligand and the addition of L′ (termed "incubation time" here) may not have been sufficient to reach an equilibrium distribution of metal-ligand species (Hering and Morel, 1988). However, multiple kinetic analysis experiments at varying incubation times can be used to test for equilibrium. Varying incubation time can also be used to study preequilibrium kinetic processes and to obtain rate constants for species transformations. For a heterogeneous ligand mixture (such as DOM), this approach can be used to determine if the metal-ligand complex dissociation rate changes with incubation time.

2.3.2. Experimental procedure

In preparation for the analysis, dry 1.00-cm optical glass cells were placed in the reference and sample beams of a Hitachi U2000 double beam UV-Vis spectrometer. The cell holder was water jacketed and maintained at 25°C using a Neslab CFT-25 refrigerated recirculator. The spectrophotometer was set to zero absorbance at 562 nm, the absorbance maxima of the iron(II)-ferrozine complex (Stookey, 1970). Fifty microliters of 50.0 mmol/L ferrozine stock (pH 6.0 or 8.0) was placed in the bottom of each of the cells, and 2.50 mL of the control
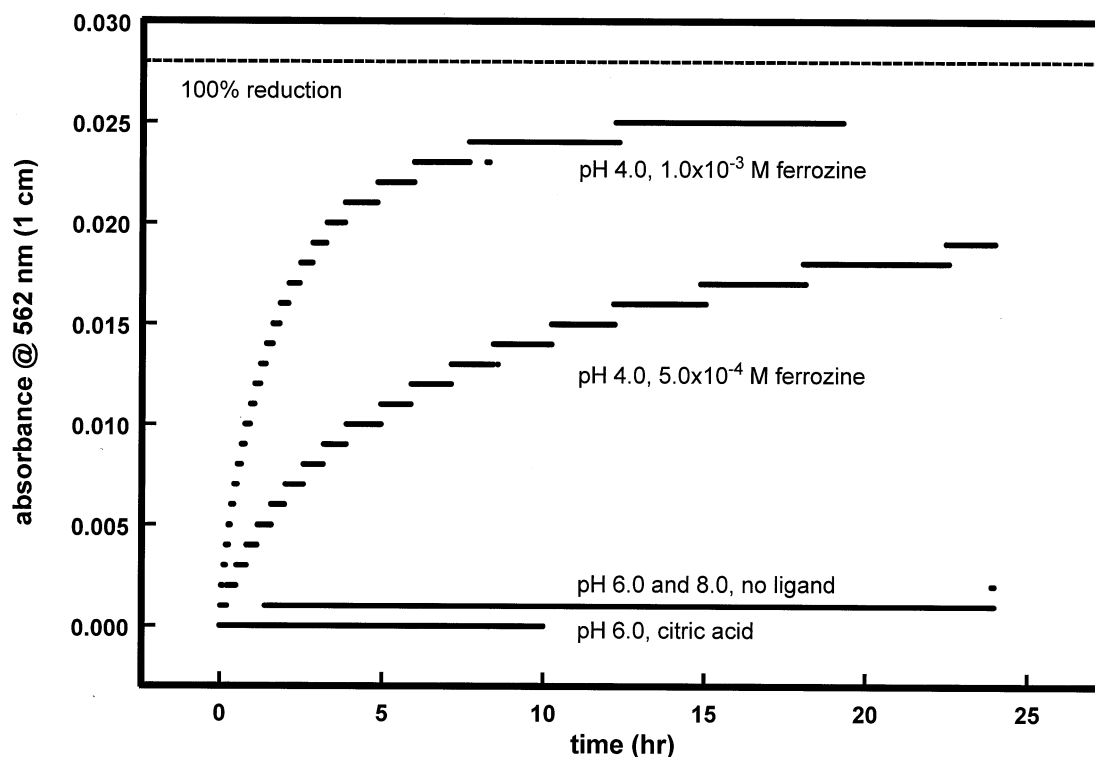
Fig. 1. The effect of pH and iron form on the reduction of iron(III) by ferrozine. One micromole per liter total iron added as iron(III). One millimole per liter ferrozine unless noted. pH 4.0 experiments used 10.0 mmol/L acetate buffer, pH 6.0 experiments used 10.0 mmol/L MES buffer, and pH 8.0 experiments used 10.0 mmol/L HEPES buffer. Note that no ferrozine induced iron(III) reduction occurs at pH 6.0 and 8.0.

solution (no iron) was added to the ferrozine in the reference cell. This provides a stable reference that accounts for variations in lamp output during the experiment as well as the small absorbance by the fulvic acid and unreacted ferrozine (in 50-fold excess of the iron).

After the desired incubation time, the kinetic analysis experiment was begun by adding 2.50 mL of the iron–fulvic acid solution to the ferrozine in the sample cell, sealing the cells with PTFE stoppers, and closing the sample compartment. The incubation time and initial absorbance reading were noted and the collection of the absorbance at 562 nm vs. time was started. For the pH 6.0 experiments, the absorbance was recorded every 12 s for 12 h. For the pH 8.0 experiments, it was recorded every 30 s for 24 h.

Experiments were conducted at pH 6.0 and 8.0, starting with either iron(II) and iron(III), and at varying incubation times which generally included 2 to 4 min, 1 to 1.5 h, 6 to 8 h, 24 to 26 h, and 44 to 56 h. The ionic strength was varied by conducting the experiments with only the 10.0 mmol/L pH buffer and with the 10.0 mmol/L buffer plus 0.10 mol/L sodium perchlorate. No visible formation of a precipitate was noted in any of the experiments.

2.3.3. Testing of the validity of the kinetic analysis methodology

Iron(III) solutions at pH 6.0 and 8.0 with no complexing ligand, where iron is assumed to be in colloidal form, and iron(III)–citric acid solutions (pH 6.0, > 99% complexation of the iron) gave no reaction with ferrozine over the time scale of the kinetic analysis experiments conducted here (Fig. 1). These control experiments demonstrate that there is no ferrozine induced reduction of iron(III) from either its colloidal or organically-complexed forms at pH 6.0 or 8.0 (Fig. 1). However, iron(III) reduction was observed to occur at pH 4.0 (Fig. 1). This is in agreement with the results of Box (1984), who observed iron reduction at pH 4.6. In general, the results presented here indicate that the use of ferrozine to measure iron(II) at pH values < 6.0 is invalid.

In this study, further experiments were limited to pH 6.0 and above, where no ferrozine induced iron(III) reduction was observed.

The observed rate of iron(II)-ferrozine complex formation in the iron–fulvic acid solutions was found to be independent of the ferrozine concentration, indicating a disjunctive pathway (see section 2.3.1). Therefore, the rate constants presented here represent the either the dissociation of iron(II) from iron(II)–fulvic acid complexes or the thermal reduction of iron(III)–fulvic acid complexes to form iron(II). It is unlikely that these observed rates arise from iron(II)–fulvic acid dissociation. Langford et al. (1977) observed that reaction of the iron–fulvic acid mixtures with 1,10 phenanthroline (another iron[II]-specific colorimetric ligand) occurred at a rate slower than they measured for iron(III) ligand exchange. Since the kinetics of iron(II) exchange are expected to be much faster than iron(III) exchange (Langford and Gray, 1965), they concluded that the reaction with 1,10 phenanthroline was the result of thermal reduction, not the ligand exchange of iron(II). Waite and Morel (1984) and Voelker et al. (1997) also assumed that this reaction was the result of thermal reduction.

Any non-organically complexed or "inorganic" iron(II) present in the sample at the start of the kinetic analysis would also react rapidly with ferrozine. This means that the iron(II)-organic complexes would be indistinguishable from inorganic iron(II) on the seconds to minutes timescale of the kinetic analysis experiments conducted here and elsewhere (Langford et al., 1977, 1981; Waite and Morel, 1984). Iron(II)–fulvic acid and inorganic iron(II) would be measured together in these kinetic analysis experiments (termed "iron[II]") as an initial jump or time zero starting point in the iron(II)-ferrozine complex concentration. Any inorganic iron(II) produced by thermal reduction after the addition of the ferrozine will be "trapped" as the iron(II)-ferrozine complex and give rise to increasing absorbance at 562 nm as a function of time. Furthermore, the measurement of trapped iron(II) as a function of time will give the actual rate of thermal reduction.

2.3.4. Kinetic analysis data interpretation

The kinetic analysis data was fit as the sum of four components, iron(II) (X), colloidal iron (C), and two iron(III)–fulvic acid species (A and B) assuming parallel reactions and distinct rate constants. (The chemical assignment of the components is discussed below.) When the data were fit using only one iron(III)-SRFA complex the fits were obviously inadequate. Using three iron(III)–fulvic acid components did not improve the goodness of fit and the increased number of parameters made the fit difficult to optimize, relative to two components. With no constraints, the inclusion of two iron(III)–fulvic acid species, iron(II), and colloidal iron in the fitting gives a total of eight adjustable parameters, four initial concentrations and four rates, to be varied to fit the data.

The independent measurement of iron(II) and colloidal iron allowed a number of these fitting parameters to be fixed during the data fitting, greatly increasing its reliability. The iron(II) concentration was estimated from the first data point measured in the kinetic analysis, fixing one parameter. The reaction rate of iron(II) with ferrozine (3.1×10^{11} mol/L^{-3} s^{-1}; Thompsen and Mottola, 1984) is instantaneous on the time scale of our experiments and is therefore not included in the fitting of our data, fixing a second parameter during the analysis. The colloid concentration vs. time data from the companion paper (Pullin and Cabaniss, 2003) were numerically fit. The resulting equations were used to calculate the iron colloid component ([C]) concentration for the desired incubation time. Since colloidal iron does not react with ferrozine (discussed below), its reaction rate is zero. This allows us to fix two more parameters in the data analysis. The total iron concentration (Fe$_T$) in the experiments is known, so that another concentration parameter is fixed by imposing mass balance. Thus, the experimental data is fit to a four component model using only three adjustable parameters, one iron–fulvic acid complex initial concentration ([A]$_0$ or [B]$_0$) and two iron–fulvic acid reaction rates (k_A and k_B). The equations defining the four component model are

$$[P]_0 = [A]_0(1 - e^{-k_A t}) + [B]_0(1 - e^{-k_B t}) + [X] \tag{3}$$

$$[A]_0 = Fe_T - [X] - [B]_0 - [C] \tag{4}$$

where the time (t) is the independent variable and the measured concentration of common product ([P]) is the dependent variable.

The data were fit by non-linear regression using Scientist (Micro-Math Software, Salt Lake City, USA) running on a PC. This program uses a modification of the Powell approach, a hybrid of the steepest descent and Gauss-Newton algorithms. Multiple initial guesses as well as refinement of these guesses using the simplex algorithm were used to guard against convergence to local minima.

The values for k_A and k_B obtained for sets of kinetic analysis data at varying incubation times, but with a single pH, ionic strength, and initial iron redox state, were similar (within a factor of 2) and varied randomly with incubation time. The non-systematic variation in the rate constants is probably due to the uncertainty in fitting (including the approximations in representing iron(III)–fulvic acid as only two complexes) rather than genuine changes in the nature of thermal reduction. The values of k_A and k_B for a given set of solution conditions were averaged for experiments with different incubation times and used to refit that group of data. During this second fitting the averaged rate constants were fixed, reducing the fitting problem to the optimization of a single linear parameter ([B]$_0$) which is completed in a single mini-mization step. This method forces all of the variation from one incubation time to another to be expressed in the species initial concentrations.

This model assumes that all of the observed change in speciation are due to shifts in iron species concentrations, not time dependent changes in the rate constants for thermal reduction. This assumption implies that iron–fulvic acid binding is the result of complexation by a set of discrete sites that do not change in binding ability over time. In a practical sense, our approach is justified by the fact that even after averaging the rate constants over incubation time reasonable fits are still obtained for the experimental data in most cases, to within a few percent of the measured data. In a few instances, the fit is notably poorer. This may indicate that our assumption of discrete sites represents an oversimplification. A more realistic description of the iron–fulvic acid interaction is probably a continuum of binding sites with a

varying affinity for iron. However, the discrete model used here represents the experimental data well and provides a simple conceptual model for understanding changes in iron reactivity over time.

4. RESULTS

In all cases, the recovery of iron as iron(II)-ferrozine, measured after 12 or 24 h, decreased as the incubation time increased (Fig. 2, Table 1). More iron was recovered at pH 6.0 than at pH 8.0, even though the pH 8.0 experiments were allowed to proceed for a longer period of time. Increased recovery was observed in the systems starting with iron(II) relative to those starting with iron(III), although this difference decreased at longer incubation times.

Ionic strength also affected the recovery of iron in the kinetic analysis experiments. When starting with iron(III), slightly lower recovery was observed for the higher ionic strength experiments (0.10 mol/L NaClO$_4$) at both pH values. The result was the same when starting with iron(II) at pH 8.0. However, when starting with iron(II) at pH 6.0 there was a much larger effect of ionic strength, giving increased recovery at the higher ionic strength experiments. Overall, the time to reach a stable value of recovery as iron(II)-ferrozine in dark iron–fulvic acid systems at near-neutral pH was > 56 h, the longest time period examined here.

To quantify the process of thermal reduction independently from the other changes in speciation occurring in solution (such as iron[II] oxidation and iron colloid formation), the data were fit to a four component model (see section 2.3.4 for details). This analysis yielded first order rate constants for the thermal reduction of iron(III) contained in two SRFA complexes, denoted A and B (Table 2). As noted in section 2.3.4, no systematic variation in the rate constants with incubation time was observed, and so the averaged values are reported here.

For a given pH, these rate constants were in good agreement for the higher and lower ionic strength experiments and for the experiments starting with iron(II) vs. starting with iron(III) (Table 2). T tests indicate that in all but one case, there was no difference in the rate constants (95% confidence level) due to ionic strength. T tests did indicate that the values of k_A and k_B for the experiments starting with iron(II) were significantly higher than those for the experiments starting with iron(III). However, when the values of k_A and k_B were averaged overall experimental conditions excepting pH (incubation time, ionic strength, and initial iron redox state) to give a single set of k_A and k_B for each pH value, reasonable fits of the experimental data could still be obtained (to within 5% of the experimental data) (Fig. 3).

In addition to the thermal reduction rate constants, the kinetic analysis also provides the concentrations of the two iron(III)-SRFA complexes (designated A and B) at a given incubation time (Tables 3 and 4). When combined with the independently measured concentrations of iron(II) and colloidal iron, the speciation of the iron can be plotted as a function of time and experimental conditions (Fig. 4). This gives a "picture" of the iron speciation as it evolves over time. Because our methodology does not discriminate between free and fulvic acid bound iron(II) (see section 2.3.3), the picture is somewhat incomplete. However, no previous report has provided such time-dependent iron speciation data.

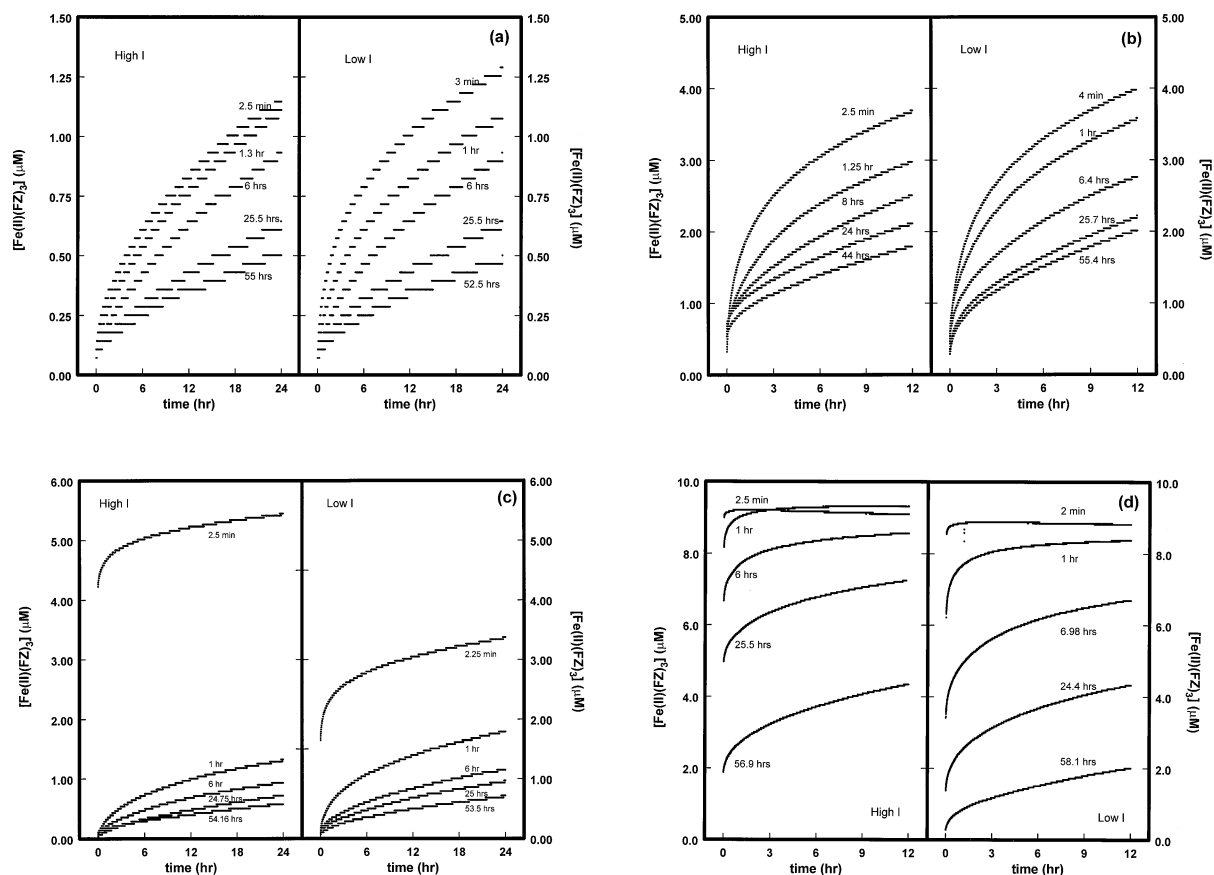Figure 4 shows an overall trend of a shift in speciation over

Fig. 2. Kinetic analysis raw data as a function of incubation time, pH, ionic strength, and initial iron redox state. 10 mg/L fulvic acid, 10.0 μmol/L iron, 10.0 mol/L pH buffer, 0.10 mol/L sodium perchlorate (high I only), labels indicate incubation time. Note that the y-axis scale varies among the four plots. (a) Iron added as iron(III) at pH 8.0. (b) Iron added as iron(III) at pH 6.0. (c) Iron added as iron(II) at pH 8.0. (d) Iron added as iron(II) and pH 6.0.

time from the faster reacting iron(II) and iron(III)–fulvic acid species (A) to the slower reacting iron(III)–fulvic acid complex (B) and colloidal iron. While the slower-reacting iron(III)-$SRFA_B$ species is usually present in higher concentration than iron(III)-$SRFA_A$, both of the iron–fulvic acid species decrease in concentration over time while the colloidal iron increases with time. An exception is at pH 6.0 starting with iron(II), where iron(III)-$SRFA_A$ increases up to the 6 h incubation time and then decreases while iron(III)-$SRFA_B$ and colloidal iron increase with time (Figs. 4d and 4e).

The time dependent speciation is affected by both the redox state of the iron at the beginning of the experiment and the solution pH (Fig. 4). Colloidal iron concentrations are higher at pH 8.0 than at pH 6.0. At pH 8.0, experiments starting with iron(II) (Fig. 4b) have higher colloidal iron concentrations with correspondingly lower iron(III)-$SRFA_B$ concentrations than those starting with iron(III) (Fig. 4a vs. Fig. 4b). At pH 6.0, the formation of the iron(III)–fulvic acid complexes and colloidal iron is considerably slower in experiments starting with iron(II) than with iron(III) (Figs. 4d and 4e vs. Fig 4c), presumably due to the slow oxidation rate at that pH (see Pullin and Cabaniss, 2003). Additionally, significant amounts of iron(II) are present even after 56 h (Figs. 4c–4e) at pH 6.0. However, at pH 8.0 no steady state iron(II) was observed (Figs. 4a and 4b). The effect

of ionic strength on the speciation data is generally very small. The exception is at pH 6.0 when starting with iron(II) (Fig. 4d vs. Fig. 4e).

Once the concentrations and thermal reduction rate constants were known for the A and B iron(III)–fulvic acid complexes, the total rate of thermal reduction was calculated (Tables 3 and 4). During the pH 8.0 experiments and the pH 6.0 experiments starting with iron(III), this rate decreased with time. However, at pH 6.0 and starting with iron(II), the thermal reduction rate initially rises over time (as iron(II) is slowly oxidized to form iron(III)) and then falls after 6 h. The overall rates of thermal reduction are approximately one order of magnitude faster at pH 6.0 than at pH 8.0 and are slightly faster at lower ionic strength (at either pH value).

4. DISCUSSION

4.1. Time Dependent Iron-DOM Speciation in Model Solutions

The use of the four component model allows us to interpret the kinetic analysis data in terms of the underlying iron speciation, including the observed shifts in recovery. Increased colloid formation over time decreases the amount of iron(III)–

Table 1. The recovery of iron as the 1:3 iron(II)-ferrozine complex in the kinetic analysis experiments.

Low I		High I	
Incubation time	Recovery (%)[a]	Incubation time	Recovery (%)[a]
pH 8.0, starting with iron(III)			
3 min	12.9	2.5 min	11.5
1 hr	10.8	1.3 hr	11.1
6 hr	9.0	6 hr	9.3
25.5 hr	6.5	25.5 hr	6.1
52.5 hr	4.7	55.06 hr	5.0
pH 8.0, starting with iron(II)			
2.25 min	33.7	2 min	54.5
1 hr	17.9	1 hr	13.3
6 hr	11.5	6 hr	9.3
25 hr	9.7	24.8 hr	7.2
53.5 hr	7.2	54.2 hr	5.7
pH 6.0, starting with iron(III)			
4 min	39.8	2.5 min	36.9
1 hr	35.8	1.25 hr	29.7
6.4 hr	27.6	8 hr	25.1
25.7 hr	22.2	24 hr	21.1
55.4 hr	20.1	44 hr	17.9
pH 6.0, starting with iron(II)			
2 min	88.2	2.5 min	91.0
1 hr	83.8	1.07 hr	93.2
6.98 hr	66.9	6 hr	85.7
24.4 hr	43.2	25.6 hr	72.4
58.1 hr	37.3	56.9 hr	43.5

[a] The amount of iron(II)-ferrozine complex, relative to total added iron, measured after 12 hr for pH 6.0 and after 24 hr for pH 8.0.

fulvic acid present to undergo thermal reduction, slowing the observed rate. Additionally, we observed a shift in iron speciation from faster to slower reacting iron(III)–fulvic acid complexes over time. Both processes act together, resulting in a decreased amount of iron recovered as iron(II)-ferrozine over time and at increasing pH. The decreased recovery of iron(II)-ferrozine at pH 8.0, relative to pH 6.0, is also partially due to a decrease in the inherent thermal reduction rate constants.

As noted earlier, no effect of ionic strength on the thermal reduction rate constants was observed. Therefore, the ionic strength effects on iron(II) oxidation, iron(III) complexation, and colloid formation are responsible for the observed differ-

Table 2. The first order rate constants, k_A and k_B, for the thermal reduction of two iron(III)-fulvic acid complexes (A and B). The values were averaged over incubation time (see text for details).

Experimental conditions		$k_A \pm 1\sigma$ (hr^{-1})	$k_B \pm 1\sigma$ (hr^{-1})
pH 8.0			
Iron(III)	High I	0.29 ± 0.10	0.0048 ± 0.0007
	Low I	0.36 ± 0.10	0.0048 ± 0.0007
Iron(II)	High I	0.41 ± 0.22	0.010 ± 0.002
	Low I	0.51 ± 0.25	0.018 ± 0.006
pH 6.0			
Iron(III)	High I	1.1 ± 0.2	0.021 ± 0.004
	Low I	1.2 ± 0.2	0.024 ± 0.002
Iron(II)	High I	1.7 ± 0.2	0.10 ± 0.04
	Low I	1.8 ± 0.4	0.064 ± 0.029

ences in speciation between the high and low ionic strength experiments. For example, the largest effect of ionic strength on the speciation data is seen at pH 6.0 when starting with iron(II) (Figs. 4d and 4e). In this system, the relatively slow oxidation of iron(II) controls the rate of formation of iron(III) and therefore the iron(III)–fulvic acid complexes and colloidal iron. Thus, the large effect of ionic strength on the oxidation rate observed earlier (Pullin and Cabaniss, 2003) is propagated through the formation of the iron(III) species and their subsequent transformations. The effect of ionic strength is much smaller under conditions where there is little iron(II), such as starting with iron(III) (Figs. 4a and 4c) or when starting with iron(II) at pH 8.0 where oxidation is relatively rapid (Fig. 4b).

There is a notable effect of pH on the thermal reduction rate constants, with the values at pH 6.0 being 2 to 4 times larger than those at pH 8.0. However, given the 100-fold change in the H^+ concentration between the two pH values, this pH dependence should not be taken as evidence for the direct involvement of H^+ in the thermal reduction reaction mechanism. One possible explanation for the pH effect is that increased pH could lead to deprotonation of partially hydrolyzed fulvic acid–bound iron(II). Analogous to the situation with inorganic iron(II) hydrolysis species, this could lead to faster reoxidation of the iron(II) complex (before dissociation to form Fe^{2+}). However, this explanation is speculative and more study on the exact mechanism of thermal reduction is clearly needed.

It is difficult to compare the thermal reduction rate constants measured here to the kinetic analysis rate constants determined by others for iron-DOM solutions. Most of the published values were determined using colorimetric reagent solutions that were either acidic or contained an added reductant (Langford et al., 1977, 1981; Tipping et al., 1982; Sojo and De Haan, 1991), conditions that induce the reduction of iron(III). While these experimental approaches still yield useful information regarding the concentrations of the iron species in the sample, the rates measured under these conditions are not for thermal reduction alone (see section 2.3.3).

An exception are the experiments of Waite and Morel (1984), who used 1,10 phenanthroline to trap thermally-reduced iron(II) without added reductant or acidification. At pH 6.5, 10 mg/L Suwannee River fulvic acid, and 0.10 mol/L NaCl they found two components that reacted with rate constants of 1.3 and 0.066 h^{-1} after a 3-h incubation time. These values are in reasonable agreement with our values of 1.1 and 0.021 h^{-1} at pH 6.0 and 0.10 mol/L NaClO$_4$ (Table 2). Similar values were observed for a fulvic acid extracted from Grassy Pond (Massachusetts), indicating that the results obtained using SRFA are not anomalous.

Overall, the results presented here and in the companion paper demonstrate that multiple iron–fulvic acid complexes can drastically alter the speciation of iron in natural waters. Clearly, complexation increases the amount of iron in the dissolved phase, relative to what would be expected in non-organic ligand containing solutions. Less obviously (but equally important), this work indicates that organic complexation permits iron(III) reduction, with slower rates at higher pH and higher rates in newly made solutions. The former effect is due both to smaller reduction rate constants and changes to speciation favoring colloid formation at pH 8.0. The latter effect is purely a
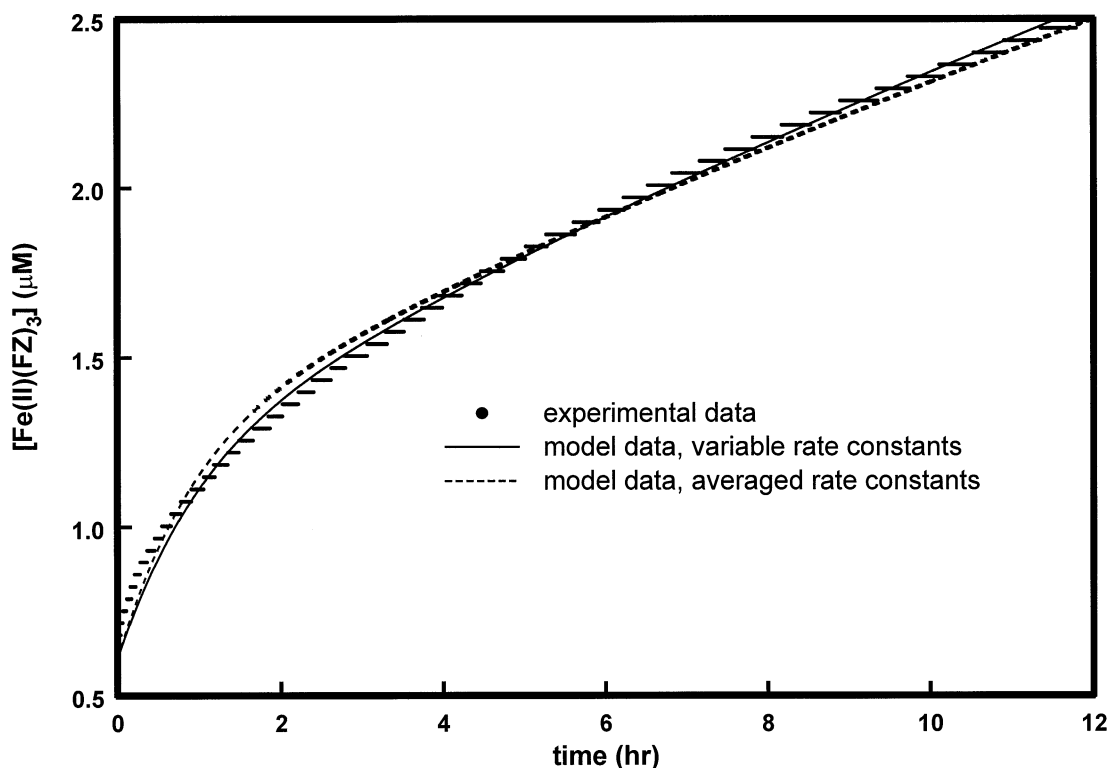
Fig. 3. An example of kinetic analysis raw (pH 6.0, iron[III], 8 h) and model data. Two fits to the experimental data are shown, before and after averaging the rate constants and refitting the data.

speciation effect, in which iron shifts to less reducible species with time.

4.2. A Conceptual Model of Iron Speciation in Humic Natural Waters

To summarize the results of this study, we propose a conceptual model of iron speciation in humic natural waters (Fig. 5). The model contains inorganic iron(II) and iron(III) (the sums of their various hydrolysis species), one iron(II)–fulvic acid species, two iron(III)–fulvic acid species (differentiated by their thermal reduction rate constants), and colloidal iron. The inclusion of two iron(III)–fulvic acid species in the model was determined by our inability to fit our kinetic analysis data using only a single species (see section 2.3.4). The colloidal iron is certainly a heterogeneous mixture, including a distribution of particle sizes and reactivities as well as some fraction of the organic material in the system. However, since our methodology only determines the total amount of colloidal iron in the system, it is represented here as one combined pool of iron. The thermal reduction of iron(III) is represented by reactions 5 and 8. While more complicated conceptual models could be postulated, we believe that this is the simplest model that can explain our laboratory results. It is important to emphasize that in real environmental systems additional reactions would be coupled with this relatively simple scheme, notably including both the photochemical and biochemical reduction of iron(III) and biologic oxidation of iron(II).

Having proposed this conceptual model, we can use it to explain the qualitative aspects of our data. For example, in the companion paper (Pullin and Cabaniss, 2003) we propose that in the presence of fulvic acid, the oxidation of Fe(II)-SRFA controls the overall rate of oxidation. In terms of the conceptual model, this would mean that the sum of reaction 3 followed by reaction 5 (reaction pathway 3, 5) is faster than reaction 1.

In a second example, one surprising result from this study is that more colloidal iron is generated in iron–fulvic acid systems that are made with iron(II) than those made with iron(III). Thermodynamically, no difference in the iron speciation between these two systems should be observed at long times (in presence of saturated O_2). Thus, our data indicate that the ratio of iron(III)–fulvic acid to colloidal iron may be controlled by a kinetic process.

This kinetic effect can not be explained if only one iron(II)–fulvic acid complex and one iron(III)–fulvic acid complex exist. However, if two iron(III)–fulvic acid complexes with different reactivities are posited in the arrangement shown in Figure 5, then the difference can be explained. If reaction pathway 3, 5 (iron[II] complexation followed by oxidation) is faster than reaction 1 (inorganic iron[II] oxidation), and reaction pathway 3, 5, 6 (conversion of iron[II] to iron[III]-SRFA$_A$ and then to colloidal iron) is faster than reaction pathway 7, 9 (conversion of iron[III] to iron[III]-SRFA$_B$ and then to colloidal iron), then starting with iron(II) could initially lead to more colloid formation than starting with iron(III). If the rates of colloid dissolution were relatively slow compared to the corresponding forward reactions, then this initial difference in

Table 3. Iron speciation as a function of time in iron–Suwannee River fulvic acid mixtures at pH 8.0. The total rate of thermal reduction is also included. Results obtained using averaged and fixed rate constants during the kinetic analysis (see text for details).

Incubation time	[Fe(II)][a] (μM)	[A]$_0$[b] (μM)	[B]$_0$[b] (μM)	[colloid][c] (μM)	Total rate of thermal reduction (μM/hr^{-1})
Iron(III), high I					
2.5 min	0.11	0.35	6.9	2.3	0.20
1.3 hr	0.11	0.35	5.9	3.2	0.19
6 hr	0.11	0.28	4.6	4.7	0.15
25.5 hr	0.11	0.091	4.0	5.4	0.073
55.06 hr	0.072	0.076	3.6	5.8	0.064
Iron(III), low I					
3 min	0.072	0.60	6.2	2.8	0.29
1 hr	0.072	0.42	5.7	3.4	0.22
6 hr	0.072	0.35	4.1	5.1	0.18
25.5 hr	0.072	0.18	3.3	6.1	0.10
52.5 hr	0.072	0.091	3.1	6.4	0.065
Iron(II), high I					
2 min	4.2	0.61	3.2	1.6	0.27
1 hr	0.072	0.58	2.8	6.1	0.25
6 hr	0.11	0.25	2.7	6.6	0.12
24.8 hr	0.072	0.17	2.0	7.3	0.086
54.2 hr	0.11	0.078	1.8	7.6	0.048
Iron(II), low I					
2.25 min	1.7	0.41	4.9	2.7	0.21
1 hr	0.15	0.65	2.5	6.3	0.28
6 hr	0.15	0.25	2.2	7.1	0.12
25 hr	0.15	0.27	1.3	7.9	0.12
53.5 hr	0.072	0.16	1.3	8.1	0.075

[a] Measured as the $t = 0$ amount of iron(II)-ferrozine during the kinetic analysis.
[b] Measured by kinetic analysis.
[c] Measured using flow injection analysis.

Table 4. Iron speciation as a function of time in iron–Suwannee River fulvic acid mixtures at pH 6.0. The total rate of thermal reduction is also included. Results obtained using averaged and fixed rate constants during the kinetic analysis (see text for details).

Incubation time	[Fe(II)][a] (μM)	[A]$_0$[b] (μM)	[B]$_0$[b] (μM)	[colloid][c] (μM)	Total rate of thermal reduction (μM/hr^{-1})
Iron(III), high I					
2.5 min	0.32	2.0	5.7	1.4	3.2
1.25 hr	0.54	1.1	6.3	1.7	1.9
8 hr	0.61	0.64	5.7	2.7	1.2
24 hr	0.68	0.32	5.4	3.2	0.75
44 hr	0.54	0.19	5.6	3.3	0.57
Iron(III), low I					
4 min	0.36	2.1	6.2	1.1	3.4
1 hr	0.54	1.4	6.4	1.3	2.4
6.4 hr	0.47	0.81	6.1	2.2	1.5
25.7 hr	0.32	0.59	5.3	3.4	1.1
55.4 hr	0.29	0.49	5.3	3.6	1.0
Iron(II), high I					
2.5 min	9.0	0.066	0.31	0.25	0.11
1.07 hr	8.2	1.1	0.055	0.32	1.6
6 hr	6.7	1.2	1.1	0.69	1.8
25.6 hr	5.0	0.99	1.7	2.0	1.5
56.9 hr	1.9	0.075	4.1	3.5	0.32
Iron(II), low I					
3 min	8.6	0.018	1.1	0.0064	0.084
1 hr	6.2	1.5	1.8	0.19	2.3
6 hr	3.4	1.6	3.4	1.2	2.5
24 hr	1.4	1.0	4.0	3.3	1.7
58.1 hr	0.79	1.4	2.3	5.1	2.2

[a] Measured as the $t = 0$ amount of iron(II)-ferrozine during the kinetic analysis.
[b] Measured by kinetic analysis.
[c] Measured using flow injection analysis.

colloid concentration would persist. This explanation is consistent with the observation that the formation of the slower-reacting iron(III)-SRFA$_B$ dominates in systems where iron(III) is the starting species (Figs. 4a and 4c) and that faster-reacting iron(III)-SRFA$_A$ is relatively higher (at least initially) in systems where iron(II) is the starting species (Figs. 4d and 4e).

4.3. Implications for Natural Systems

This study indicates that environmental conditions will determine the importance of thermal reduction in natural waters. Our results indicate that the inherent rate constants for thermal reduction increase as the pH falls. Taken together with the strong pH dependence on iron(III) hydrolysis and the observation that thermal reduction does not act on iron colloids, our results show that thermal reduction should be more important at relatively low pH values. While our results show that the rate of thermal reduction falls over time, this process will be mediated by daylight-induced shifts in iron speciation in many natural systems. Photoreduction of iron colloids and iron(III)-DOM complexes will shift the iron speciation back to iron(II), restarting the slow shift of the iron species to slow-reacting species.

Many studies of iron speciation in freshwater systems have

described the photochemical reduction of iron(III), followed by the oxidation of Fe(II) in the dark (often biologically-mediated) (McMahon, 1969; Miles and Brezonik, 1981; Collienne, 1983; Waite and Morel, 1984; McKnight and Bencala, 1988; McKnight et al., 1988; Sulzberger et al., 1990; Voelker et al., 1997; Sivan et al., 1998; Emmenegger et al., 2001; McKnight et al., 2001). However, it is important to realize that these observations are only the net product of the redox cycle. For example, our results show that in the absence of light, significant iron(III) reduction occurs at pH 8.0, even though no net iron(II) is ever observed. Additionally, this thermal reduction may determine the iron-speciation on which photochemical and biochemical processes act. For example, Waite and Morel (1984) found that one of two iron(III)–fulvic acid species they measured by kinetic analysis was reduced in concentration during light irradiation, suggesting that it underwent direct photochemical reaction.

While differences in experimental methods and environmental conditions make direct comparison difficult, it is clear from these studies that rates of iron reduction due to photochemical processes are considerably faster than the rates of thermal reduction measured here. However, in subsurface systems or systems where light penetration is relatively small due to high turbidity or strong absorbance by organic matter, thermal reduction may be the primary mechanism that drives iron redox
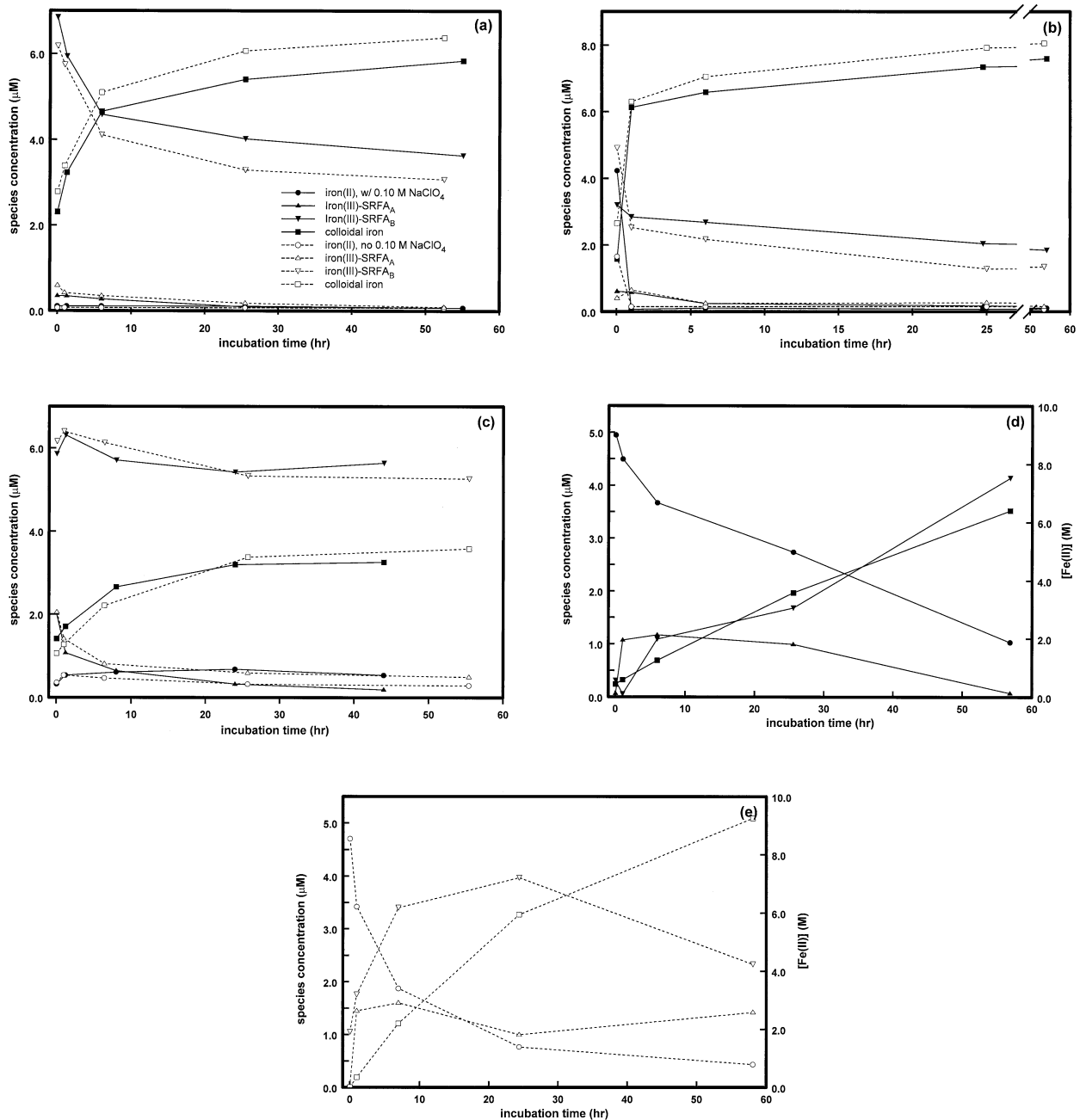
Fig. 4. Iron–Suwannee River fulvic acid speciation data as a function of incubation time as measured by kinetic analysis and flow injection analysis. 10 mg/L fulvic acid, 10.0 μmol/L total iron, 10.0 mol/L pH buffer, 0.10 mmol/L sodium perchlorate (as noted). Lines directly connect the data points for clarity only. Note that the y-axis scale varies among the five plots. (a) Iron added as iron(III) at pH 8.0. (b) Iron added as iron(II) at pH 8.0. (c) Iron added as iron(III) at pH 6.0. (d) Iron added as iron(II) at pH 6.0, high ionic strength. Iron(II) uses the right y-axis while the remaining species use the left y-axis. (e) Iron added as iron(II) at pH 6.0, low ionic strength. Iron(II) uses the right y-axis while the remaining species use the left y-axis.

cycling. Even in surface waters with significant illumination, thermal reduction may be important during the night or when significant mixing below the photic zone occurs. For example, there have been reports of night time or predawn increases of iron(II) in acidic systems (McKnight and Bencala, 1988; Wieder, 1994; Sullivan et al., 1998; Sullivan and Drever, 2001). This was attributed to biologic iron(III) reduction and/or

sulfide (pyrite) oxidation, but could have also been due to the thermal reduction of iron(III). Additionally, several studies in alkaline systems have reported night time increases dissolved and/or particulate iron concentrations (Brick and Moore, 1996; Goulet and Pick, 2001), possibly due to thermal reduction of iron(III) to iron(II) followed by the rapid reoxidation and precipitation expected at that pH range.
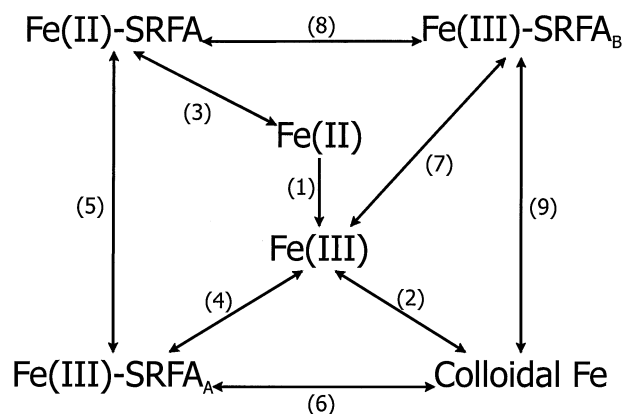
Fig. 5. A conceptual model of iron speciation and transformations in humic natural waters. This diagram represents the simplest possible situation that could explain the data presented here. It ignores additional reactions, including photochemical and biochemical processes, that could occur in the environment. (1) The oxidation of dissolved inorganic iron(II) to form dissolved inorganic iron(III) (see mechanism in introduction). The reverse reaction is negligible in the dark. The exact iron(II) and iron(III) species in this reaction depends on the pH and the identity and concentration of inorganic anions in solution. A variety of iron(II) species could undergo oxidation simultaneously, all with different rate constants. (2) The formation of colloidal iron from dissolved inorganic iron(III) and the reverse dissolution reaction. (3) The complexation of dissolved iron(II) by SRFA to form iron(II)-SRFA and the reverse dissociation reaction. (4) The complexation of dissolved iron(III) by SRFA to form iron(III)-SRFA$_A$ and the reverse dissociation reaction. (5) The oxidation of Fe(II)-SRFA to form Fe(III)-SRFA$_A$ and the reverse thermal reduction reaction. (6) The formation of colloidal iron from Fe(III)-SRFA$_A$ and the reverse dissolution reaction. (7) The complexation of dissolved iron(III) by SRFA to form iron(III)-SRFA$_B$ and the reverse dissociation reaction. (8) The oxidation of Fe(II)-SRFA to form Fe(III)-SRFA$_B$ and the reverse thermal reduction reaction. (9) The formation of colloidal iron from Fe(III)-SRFA$_B$ and the reverse dissolution reaction.

Thermal redox cycling may also influence the bioavailability of iron and phosphorous in freshwater systems. Primary and secondary biologic production are not thought to be directly limited by iron in most freshwater systems, although some exceptions have been claimed (Jackson and Hecky, 1980; Twiss et al., 2000). However, the strong phosphate binding affinity of iron(III) colloids can have a large effect on the speciation of phosphorus, which is typically the limiting nutrient in freshwater lakes. Our work demonstrates that the extent and rate of formation of these iron(III)-colloids is drastically affected by iron-DOM interactions.

Using gel-filtration chromatography and radioisotopes, a series of studies have concluded that a DOM-iron(III)-PO$_4$ complex exists in some humic freshwaters (Jones et al., 1988, 1993; Cotner and Heath, 1990; Shaw et al., 2000). Additionally, the simultaneous light-induced formation of both iron(II) and orthophosphate (the biologically active phosphorus species) has been demonstrated in some humic lake waters (Francko and Heath, 1982; Cotner and Heath, 1990). This observation has been postulated to be the result of photoreduction of the iron in the DOM-Fe-P complex (Francko and Heath, 1982; Cotner and Heath, 1990; Maranger and Pullin, 2002). Thermal reduction of iron(III) could also be a mechanism for the release of phosphate in systems where this complex occurs, thereby indirectly af-

fecting biological productivity. This would be especially true in systems such as eutrophic lakes, where the extensive biological reduction of iron(III) colloids in the anoxic sediments is disconnected from the photic zone by thermal stratification.

5. CONCLUSIONS

1. The rate of thermal reduction of iron(III) to iron(II) can be measured by ferrozine trapping of the product at pH values ≥ 6.0, since ferrozine does not "induce" iron(III) reduction and the overall reaction rate is independent of the ferrozine concentration. However, at pH 4.0 ferrozine-induced iron(III) reduction does occur, limiting the kinetic analysis method to the determination of iron species concentrations only.

2. The rate of thermal reduction in iron–fulvic acid mixtures slows with increased incubation time up to the limits of this study (~50–60 h elapsed between the addition of iron to fulvic acid solutions and the subsequent addition of ferrozine). More stable and less reducible iron(III) species, including iron(III) colloids, are favored at the longer incubation times, while the initial products of iron mixing with fulvic are more easily reduced.

3. The rates of thermal reduction are faster and the apparent rate constants are higher at pH 6.0 than at pH 8.0. Consequently, the amount of iron(II) remaining in solution after ~50 h of incubation at pH 6.0 (3–19%, depending on conditions) is 10-fold higher than at pH 8.0 (0.7–1.1%). This pH effect is due to both changes in the rate constants for thermal reduction and in the amount of reducible iron(III)–fulvic acid complexes.

4. Ionic strength affects the overall thermal reduction rate significantly but indirectly, through the iron(II) oxidation and iron(III) colloid formation reactions. Ionic strength does not directly affect the thermal reduction rate constants.

5. The redox state of the iron at the time of mixing with fulvic acid affects the iron speciation for periods up to the limits of this study (~50–60 h). This indicates that in a typical diurnal cycle, the thermal period following exposure to sunlight is not long enough to reach steady state with respect to iron redox state and complexation.

REFERENCES

Box J. D. (1984) Observations on the use of iron(II) complexing agents to fractionate the total filterable iron in natural water samples. *Water Res.* **18**, 397–402.

Brick C. M. and Moore J. N. (1996) Diel variation of trace metals in the Upper Clark Fork River, Montana. *Environ. Sci. Technol.* **30**, 1953–1960.

Cabaniss S. E. (1990) pH and ionic strength effects on nickel-fulvic acid dissociation kinetics. *Environ. Sci. Technol.* **24**, 583–588.

Collienne R. H. (1983) Photoreduction of iron in the epilimnion of acidic lakes. *Limnol. Oceanogr.* **28**, 83–100.

Cotner J. B. and Heath R. T. (1990) Iron redox effects on photosensitive phosphorus release from dissolved humic materials. *Limnol. Oceanogr.* **35**, 1175–1181.

Emmenegger L., Schönenberger R., Sigg L., and Sulzberger B. (2001) Light-induced redox cycling of iron in circumneutral lakes. *Limnol. Oceanogr.* **46**, 49–61.

Francko D. A. and Heath R. T. (1982) UV-sensitive complex phosphorus: Association with dissolved humic material and iron in a bog lake. *Limnol. Oceanogr.* **27**, 564–569.

Goulet R. R. and Pick F. R. (2001) Diel changes in iron concentrations in surface-flow constructed wetlands. *Water Sci. Technol.* **44**, 421–426.

Hering J. G. and Morel F. M. M. (1988) Kinetics of trace metal complexation: Role of alkaline-earth metals. *Environ. Sci. Technol.* **22**, 1469–1478.

Hering J. G. and Morel F. M. M. (1990) Kinetics of trace metal complexation: Ligand-exchange reactions. *Environ. Sci. Technol.* **24**, 242–252.

Jackson T. A. and Hecky R. E. (1980) Depression of primary productivity by humic matter in lake and reservoir waters of the Boreal Forest zone. *Can. J. Fisheries Aquat. Sci.* **37**, 2300–2316.

Jones R. I., Salonen K., and De Haan H. (1988) Phosphorus transformations in the epilimnion of humic lakes: Abiotic interactions between dissolved humic materials and phosphate. *Freshwater Biol.* **19**, 357–369.

Jones R. I., Shaw P. J., and De Haan H. (1993) Effects of dissolved humic substances on the speciation of iron and phosphate at different pH and ionic strength. *Environ. Sci. Technol.* **27**, 1052–1059.

Langford C. H. and Gray H. B. (1965) *Ligand Substitution Processes.* W. A. Benjamin Inc.

Langford C. H. and Khan T. R. (1975) Kinetics and equilibrium of binding of Fe^{3+} by a fulvic acid: A study by stopped flow methods. *Can. J. Chem.* **53**, 2979–2984.

Langford C. H., Wong S. M., and Underdown A. W. (1981) The interaction of a soil fulvic acid with precipitating hydrous ferric oxide at pH = 6. *Can. J. Chem.* **59**, 181–186.

Langford C. H., Kay R., Quance G. W., and Khan T. R. (1977) Kinetic analysis applied to iron in a natural water model containing ions, organic complexes, colloids, and particles. *Anal. Lett.* **10**, 1249–1260.

Maranger R, Pullin M. J (2002) *Elemental complexation by dissolved organic matter in lakes: Implications for Fe speciation and the bioavailability of Fe and P.* In *Dissolved Organic Matter in Aquatic Ecosystems* (eds. S. Findlay and R. Sinsabaugh). Academic Press, San Diego, CA.

McKnight D. and Bencala K. E. (1988) Diel variations in iron chemistry in acidic stream in the Colorado Rocky Mountains, U.S.A. *Arctic Alpine Res.* **20**, 492–500.

McKnight D. M., Kimball B. A., and Bencala K. E. (1988) Iron photoreduction and oxidation in an acidic mountain stream. *Science* **240**, 637–640.

McKnight D. M., Kimball B. A., and Runkel R. L. (2001) pH dependence of iron photoreduction in a rocky mountain stream affected by acid mine drainage. *Hydrol. Proc.* **15**, 1979–1992.

McMahon J. W. (1969) The annual and diurnal variation in the vertical distribution of acid soluble ferrous and total iron in a small dimictic lake. *Limnol. Oceanogr.* **14**, 357–367.

Miles C. J. and Brezonik P. L. (1981) Oxygen consumption in humic-colored waters by a photochemical ferrous-ferric catalytic cycle. *Environ. Sci. Technol.* **19**, 1089–1095.

Olsen D. L. and Shuman M. S. (1985) Copper dissociation from estuarine humic materials. *Geochim. Cosmochim. Acta* **49**, 1371–1375.

Pullin M. J. and Cabaniss S. E. (2003) The effects of pH, ionic strength, and iron–fulvic acid interactions on the kinetics of non-photochemical iron transformations. I. Iron(II) oxidation and iron colloid formation. *Geochim. Cosmochim. Acta* **67**, 0000–0000.

Ridder G. M. and Margerum D. W. (1977) Simultaneous kinetic analysis of multicomponent mixtures. *Anal. Chem.* **49**, 2090–2098.

Scott D. T., McKnight D. M., Blunt-Harris E. L., Kolesar S. E., and Lovley D. R. (1998) Quinone moieties act as electron acceptors in the reduction of humic substances by humics-reducing microorganisms. *Environ. Sci. Technol.* **32**, 2984–2989.

Shaw P. J., Jones R. I., and De Haan H.. (2000) The influence of humic substances on the molecular weight distributions of phosphate and iron in epilimnetic lake waters. *Freshwater Biol.* **45**, 383–393.

Sivan O., Erel Y., Mandler D., and Mishri A. (1998) The dynamic redox chemistry of iron in the epilimnion of Lake Kinneret (Sea of Galilee). *Geochim. Cosmochim. Acta* **62**, 565–576.

Sojo L. E. and De Haan H. (1991) Multicomponent kinetic analysis of iron speciation in humic Lake Tjeukemeer: Comparison of fulvic acid from the drainage basin and lake water samples. *Environ. Sci. Technol.* **25**, 935–939.

Stookey L. L. (1970) Ferrozine, a new spectrophotometric reagent for iron. *Anal. Chem.* **42**, 779–781.

Stumm W. and Morgan J. J. (1981) Aquatic Chemistry: An Introduction Emphasizing Chemical Equilibria in Natural Waters. John Wiley, New York.

Sullivan A. B. and Drever J. I. (2001) Spatiotemporal variability in stream chemistry in a high-elevation catchment affected by mine drainage. *J. Hydrol.* **252**, 237–250.

Sullivan A. B., Drever J. I., and McKnight D. M. (1998) Diel variations in element concentrations, Peru Creek, Summit County, Colorado. *J. Geochem. Explor.* **64**, 141–145.

Sulzberger B., Schnorr J. L., Giovanoli R., Hering J. G., and Zobrist J. (1990) Biogeochemistry of iron in an acidic lake. *Aquat. Sci.* **52**, 56–74.

Thompsen J. C. and Mottola H. A. (1984) Kinetics of the complexation of iron(II) with ferrozine. *Anal. Chem.* **56**, 755–757.

Tipping E., Woof C., and Ohnstad M. (1982) Forms of iron in the oxygenated waters of Esthwaite Water, U.K. *Hydrobiologia* **92**, 383–393.

Twiss M. R., Auclair J.-C., and Charlton M. N. (2000) An investigation into iron-stimulated phytoplankton productivity in epipelagic Lake Erie during thermal stratification using trace metal clean techniques. *Can. J. Fisheries Aquat. Sci.* **57**, 86–95.

Voelker B. M. and Sulzberger B. (1996) Effects of fulvic acid on Fe(II) oxidation by hydrogen peroxide. *Environ. Sci. Technol.* **30**, 1106–1114.

Voelker B. M., Morel F. M. M., and Sulzberger B. (1997) Iron redox cycling in surface waters: Effects of humic substances and light. *Environ. Sci. Technol.* **31**, 1004–1011.

Waite T. D. and Morel F. M. M. (1984) Ligand exchange and fluorescence quenching studies of the fulvic acid-iron interaction. *Anal. Chim. Acta* **162**, 263–274.

Weider R. K. (1994) Diel changes in iron(III)/iron(II) in effluent from constructed acid mine drainage treatment wetlands. *J. Environ. Qual.* **23**, 730–738.